Supporting Information

Multimodal Imaging of Amyloid Plaques: Fusion of the Single-probe Mass Spectrometry Image and Fluorescence Microscopy Image

Xiang Tian[1], Boer Xie[2], Zhu Zou[1], Yun Jiao[2], Li-En Lin[3], Chin-Lin Chen[3], Cheng-Chih Hsu[3], Junmin Peng*[2], Zhibo Yang*[1]

[1]Department of Chemistry and Biochemistry,

University of Oklahoma

101 Stephenson Parkway

Norman, Oklahoma, 73019, USA

[2]Departments of Structural Biology and Developmental Neurobiology,

Center for Proteomics and Metabolomics

St. Jude Children's Research Hospital

262 Danny Thomas Place

Memphis, Tennessee, 38105, USA

[3] Department of Chemistry, National Taiwan University,

Taipei 10617, Taiwan

Technique details in the mass spectrometry imaging (MSI) data analysis.

1. Data Pre-processing

Data pre-processing, including smoothing, peak identification, noise removal, peak alignment, and normalization, was performed using Bioinformatics Toolbox, which is a built-in function of MATLAB. The spectral profile smoothing was carryout using Savitzky-Golay filtering, and the parameters are 7-point (equivalent to a median of 0.0309 m/z) span and the degree of two. Noise peaks were determined using median absolute deviation (MAD) function, and peaks were excluded if their signal-to-noise ratio (SNR) was lower than five. The 'mspeaks' function was used for peak picking, and the first derivatives of the spectral profiles were utilized for peak assignment. Then, the 'mspalign' command was employed for peak alignment, and the default estimation method, histogram, was utilized to determine peak locations.

2. Single-probe Mass Spectrometry Imaging details

Experimental details of the Single-probe MSI technique have been previously discussed (Reference #45), and additional details of the current studies are some provided here. During the MSI experiment, the Single-probe tip is positioned slightly above the tissues surface (a few μm) to avoid direct contact, and then continuously scans over the tissue surface at a raster speed (i.e., movement velocity of the tissue sample) of 10 μm/s. The data acquisition time for each mass spectrum (i.e., dwell time) is about 0.85 s, and the line spacing is 20 μm. Thus, the sampling spot size (i.e., pixel size) is about 8.5 μm X 20 μm. The dimension of the imaging area on tissue slices is 1 mm X 0.3 mm and 0.5 mm X 0.5 mm in the positive and negative ion modes, respectively. Depending on target area, completing each MSI measurement generally requires 2 to 4 hours.

3. Image Fusion

Image fusion was conducted using Molecular Image Fusion software package developed by Caprioli *et al*. (Reference #43). Six files needed in the fusion processing include microscopy fluorescence image data, microscopy fluorescence image information, MS image data, MS image information, fusion parameters, and registration information. Among these files, microscopy image data were processed using in-house developed MATLAB script, which can extract the location information and RGB values from each pixel. The microscopy information includes the pixel number, spatial grid size and resolution. The mass spectrometry image data matrix was generated as mentioned in the method section. The MSI information includes the number of pixels, spatial grid size, resolution, and the number of metabolites. The fusion parameters were largely adopted from the default settings, except that the "height filter" was changed to 1000 to generate fusion figure of low-intensity metabolites. Registration information was generated using in-house developed MATLAB script to accurately correlate the MS image to the microscopy fluorescence image.

4. Data analysis

For positive ion mode mass spec imaging result, three plaques were chosen and for negative ion mode mass spec imaging, two plaques were chosen. The imaging experiment was only performed once in each ion mode (positive and negative). To determine the metabolites which have significant difference between plaque and surrounding region. All the pixels represent in each plaque or surrounding region were selected and generated the averaged spectra respectively. The relative intensity was obtained by normalizing to the total ion current (TIC). The error bar was the standard deviation of the relative intensity in the selected pixels and the pixel selection details were provided in the Table S1.

Supplementary Figures

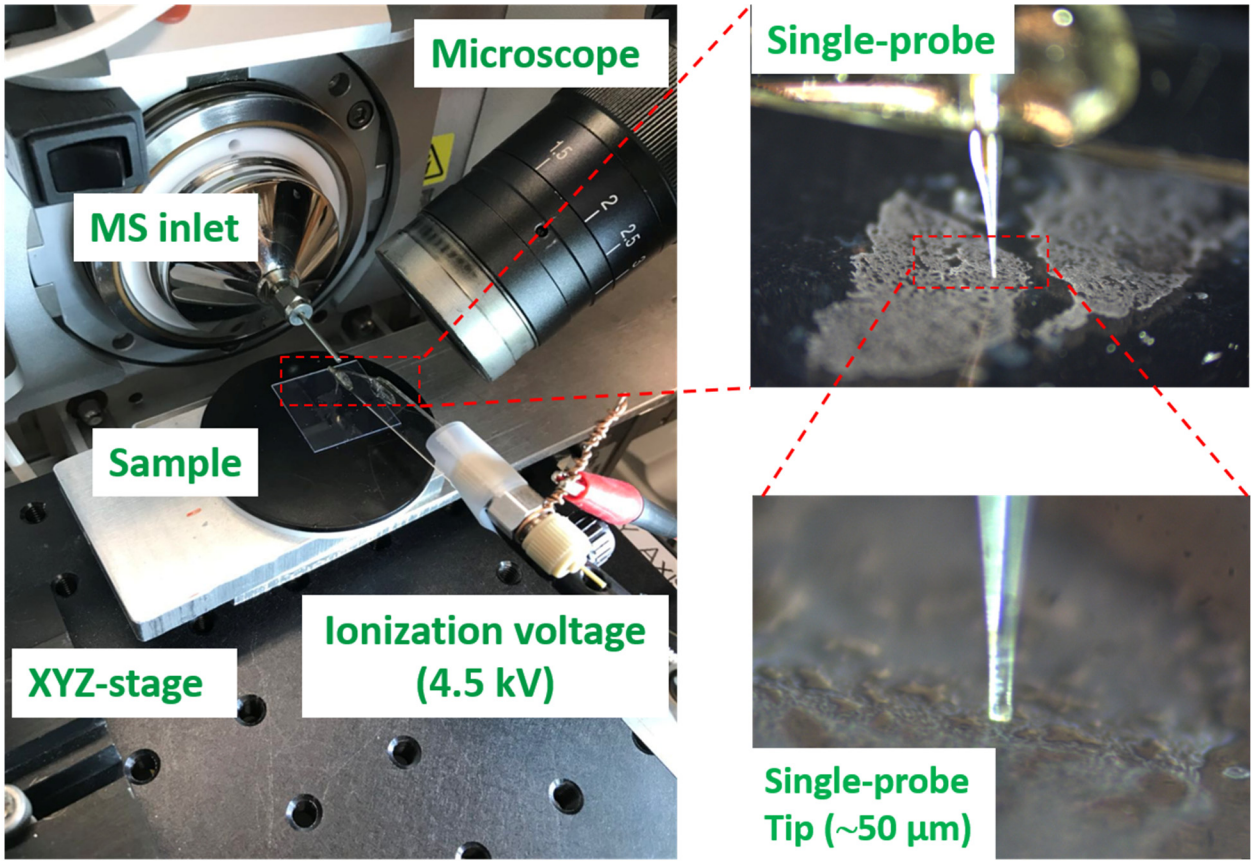

Figure S1. The Single-probe MSI experimental set-up with key components labeled.

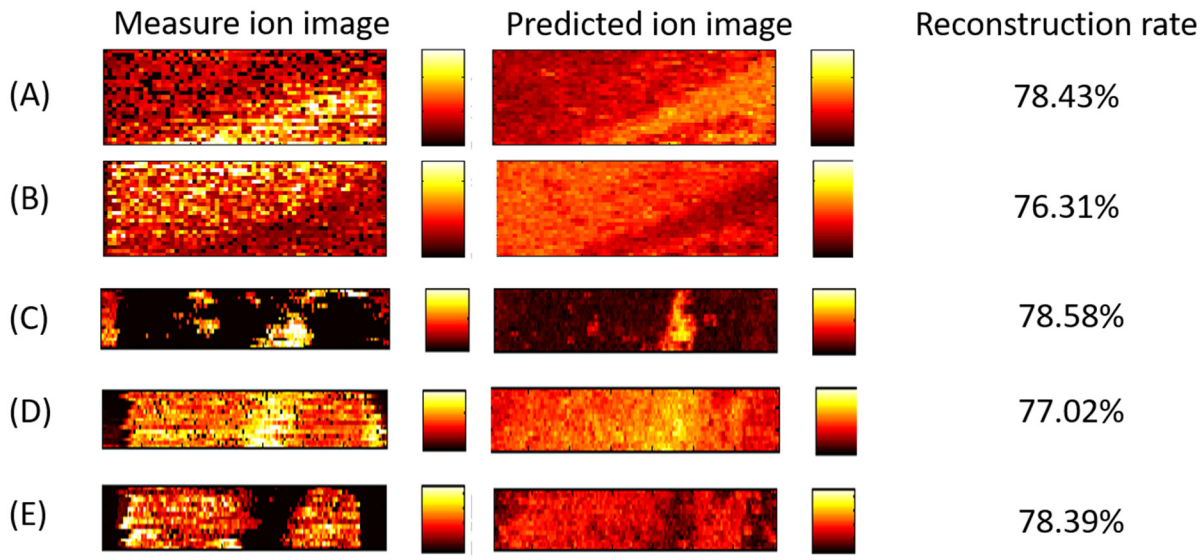

Figure S2. The reconstruction rate obtained from measured MS images (left) and predicted images (right) for selected ions, including (A) $[PA(O\text{-}32:0) - 2H]^{2-}$ (m/z 309.2514), (B) $[Dodecenoic\ acid + K - 2H]^{-}$ (m/z 251.1053), (C) $[LPC(18:0) + H]^{+}$ (m/z 524.3696), (D) $[PC(34:1) + H]^{+}$ (m/z 760.5851), and (E) $[PC(38:6) + K]^{+}$ (m/z 844.5218). All metabolites were identified using MS/MS from tissue slice, and results were compared with METLIN.

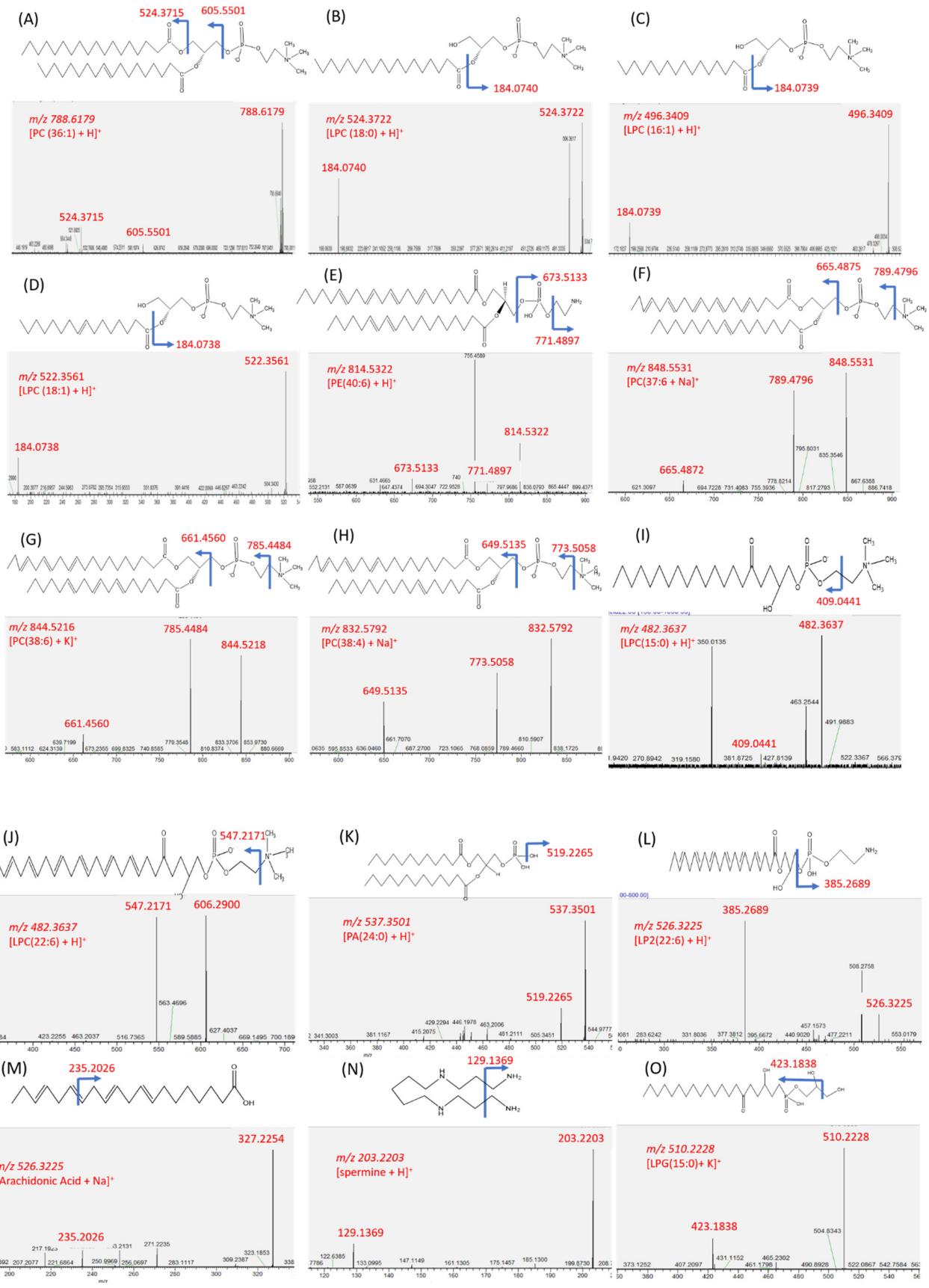
(A)
524.3715
605.5501
m/z 788.6179
[PC (36:1) + H]+
788.6179
524.3715
605.5501
(B)
184.0740
m/z 524.3722
[LPC (18:0) + H]+
524.3722
184.0740
(C)
184.0739
m/z 496.3409
[LPC (16:1) + H]+
496.3409
184.0739
(D)
184.0738
m/z 522.3561
[LPC (18:1) + H]+
522.3561
184.0738
(E)
673.5133
771.4897
m/z 814.5322
[PE(40:6) + H]+
814.5322
673.5133
771.4897
(F)
665.4875
789.4796
m/z 848.5531
[PC(37:6 + Na]+
848.5531
789.4796
665.4872
(G)
661.4560
785.4484
m/z 844.5216
[PC(38:6) + K]+
785.4484
844.5218
661.4560
(H)
649.5135
773.5058
m/z 832.5792
[PC(38:4) + Na]+
832.5792
773.5058
649.5135
(I)
409.0441
m/z 482.3637
[LPC(15:0) + H]+
482.3637
409.0441
(J)
547.2171
606.2900
m/z 482.3637
[LPC(22:6) + H]+
547.2171
606.2900
563.4696
(K)
519.2265
m/z 537.3501
[PA(24:0) + H]+
537.3501
519.2265
(L)
385.2689
m/z 526.3225
[LP2(22:6) + H]+
385.2689
526.3225
(M)
235.2026
m/z 526.3225
[Arachidonic Acid + Na]+
327.2254
235.2026
(N)
129.1369
m/z 203.2203
[spermine + H]+
203.2203
129.1369
(O)
423.1838
m/z 510.2228
[LPG(15:0)+ K]+
510.2228
423.1838

Figure S3. MS/MS analysis of selected metabolites (in the positive ion mode), including (A) [PC(36:1) + H]$^+$, (B) [LPC(18:0) + H]$^+$, (C) [LPC(16:1) + H]$^+$, (D) [LPC(18:1) +H]$^+$, (E) [PE(40:0) + H]$^+$, (F) [PC(37:6) + Na]$^+$, (G) [PC(38:6) + K]$^+$, (H) [PC(38:4) + Na]$^+$, (I) [LPC(15:0 + H)]$^+$, (J) [LPC(22:6) + H]$^+$, (K) [PA(24:0) + H]$^+$, (M) [Arachidonic acid + Na]$^+$, (N) [Spermine + H]$^+$, and (O) [LPG(15:0) + K]$^+$(All MS/MS spectra were compared with online databases METLIN).

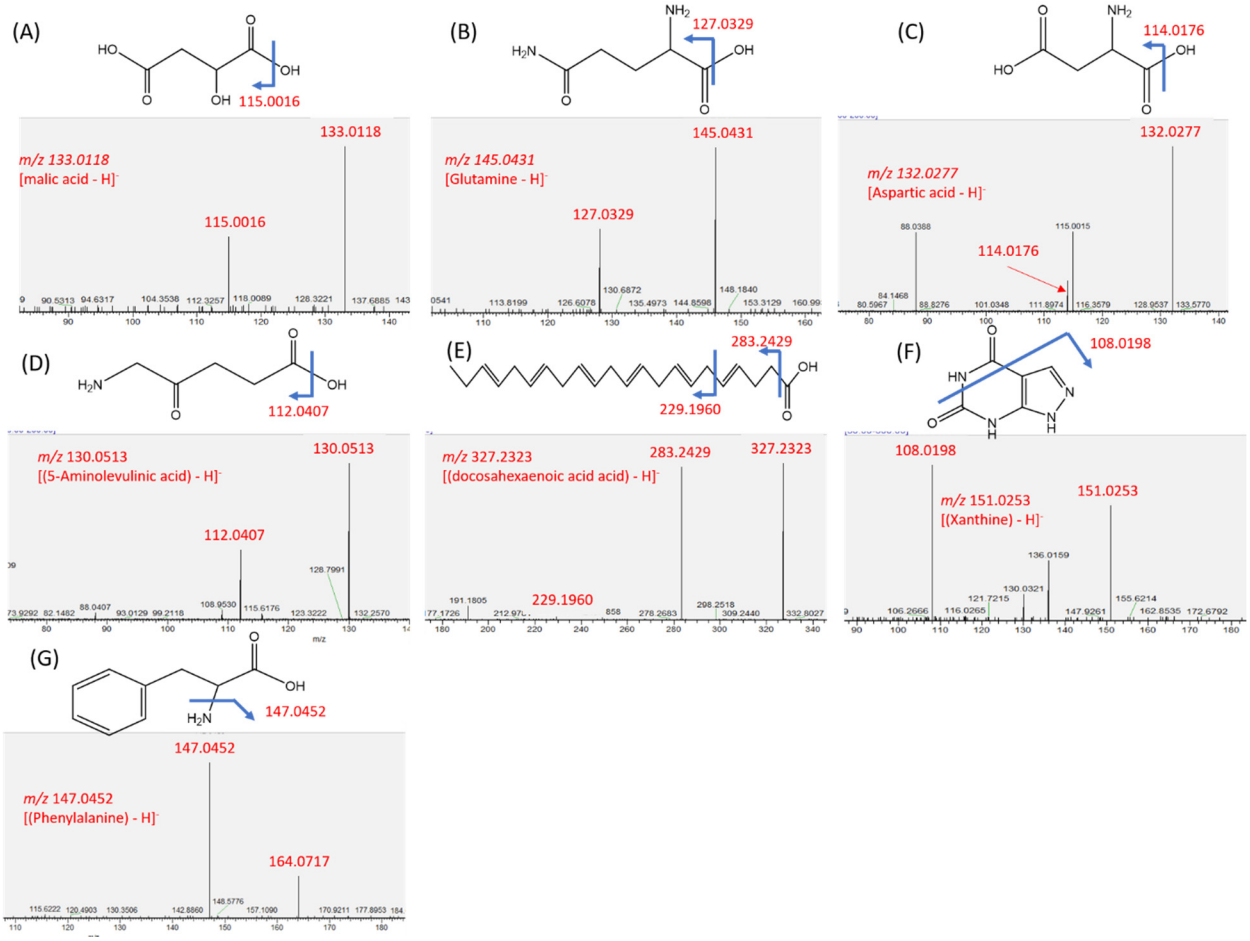

Figure S4. MS/MS analysis of selected metabolites (in negative ion mode), including (A) [malic acid - H]$^-$, (B) [glutamine - H]$^-$, (C) [aspartic acid - H]$^-$, (D) [5-aminolevulinic acid - H]$^-$, (E) [docosahexaenoic acid - H]$^-$, (F) [Xanthine - H]$^-$, and (G) [Phenylalanine - H]$^-$. (All MS/MS spectra were compared with online databases METLIN).

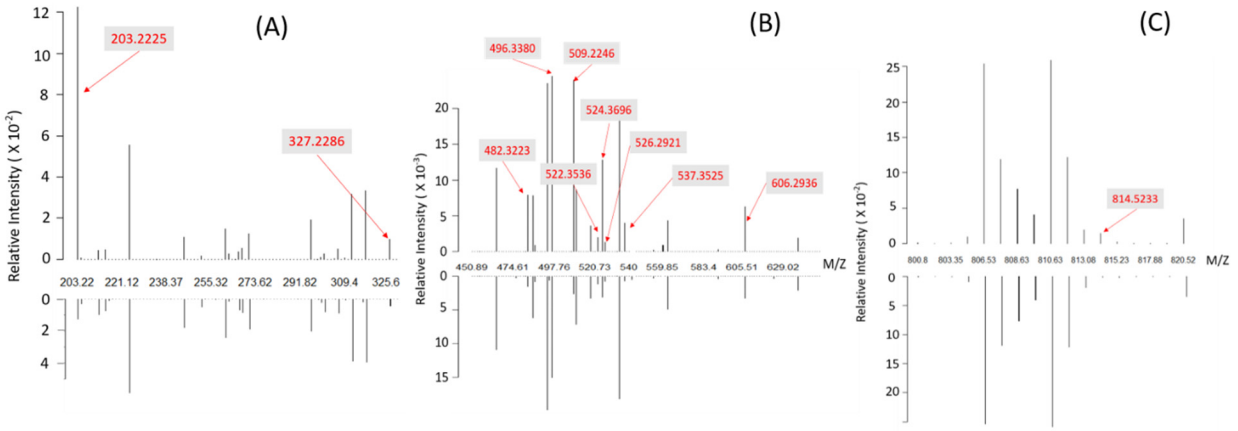

Figure S5. Zoomed-in average mass spectra of Figure 4B illustrating metabolites with significantly different abundances between Aβ plaque (Plaque 1) and its surrounding region. Mass spectra in zoomed-in ranges of (A) 200 to 330 m/z, (B) 450 to 630 m/z, and (C) 800 to 820 m/z.

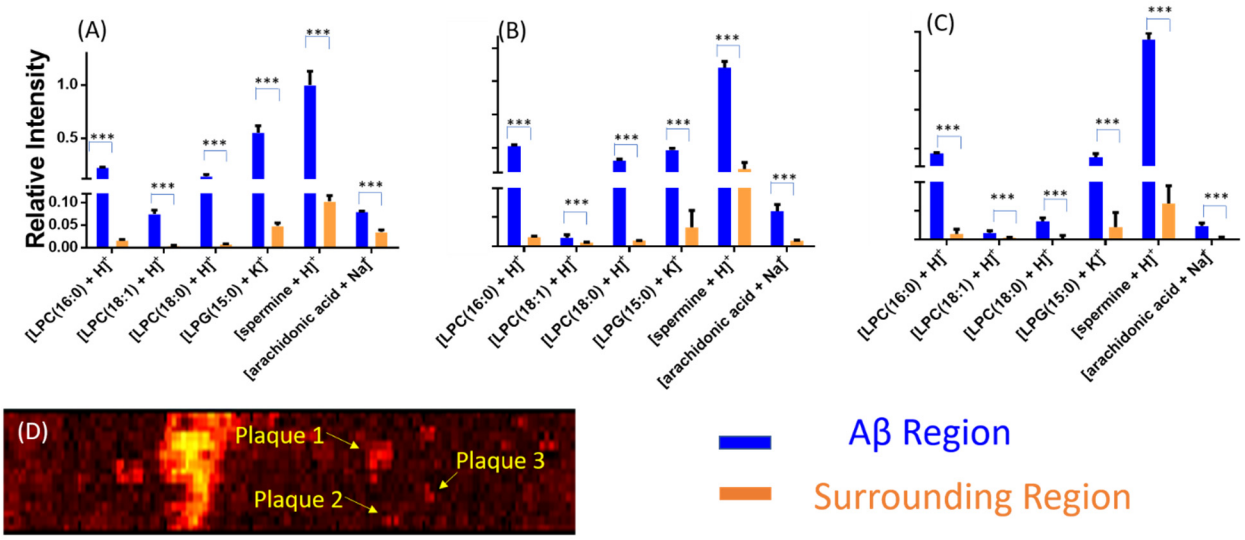

Figure S6. Metabolites with significantly different abundances between Aβ plaques and their surrounding regions. Results were obtained from (A) Plaque 1, (B) Plaque 2, and (C) Plaque 3. (D) Three selected plaques shown in the fused image. All metabolites were identified using MS/MS on tissue slice, and results were compared with database METLIN. (From t-test: ***, $P < 0.001$).

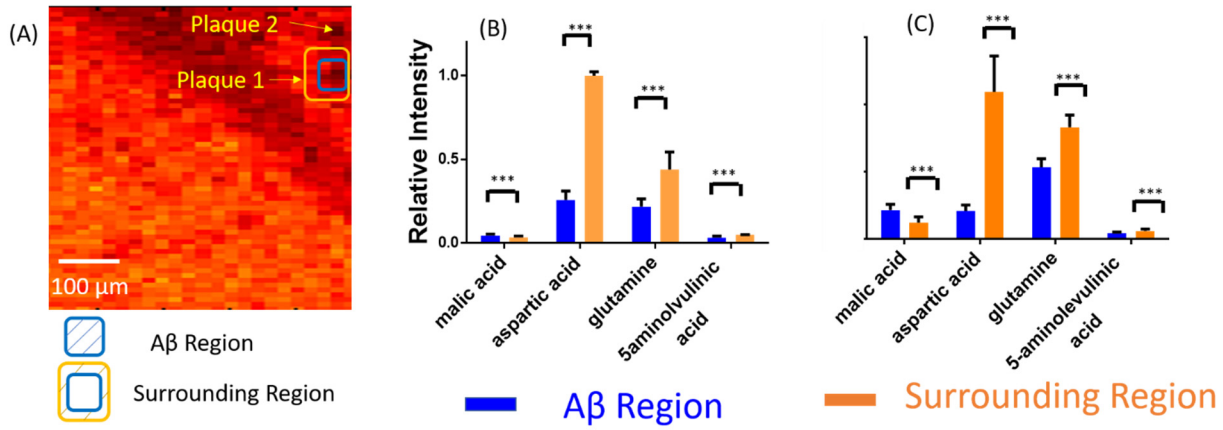

Figure S7. Pixels selection and comparison of relative ion intensities. (A) Pixels selection of Aβ plaques and their surrounding areas based on the fused image. Metabolites possessing significantly different abundances between Aβ plaques and their surrounding regions measured from (B) Plaque 1 and (C) Plaque 2. All metabolites were identified using MS/MS on tissue slice, and results were compared with database METLIN. (From t-test: ***, < 0.001)

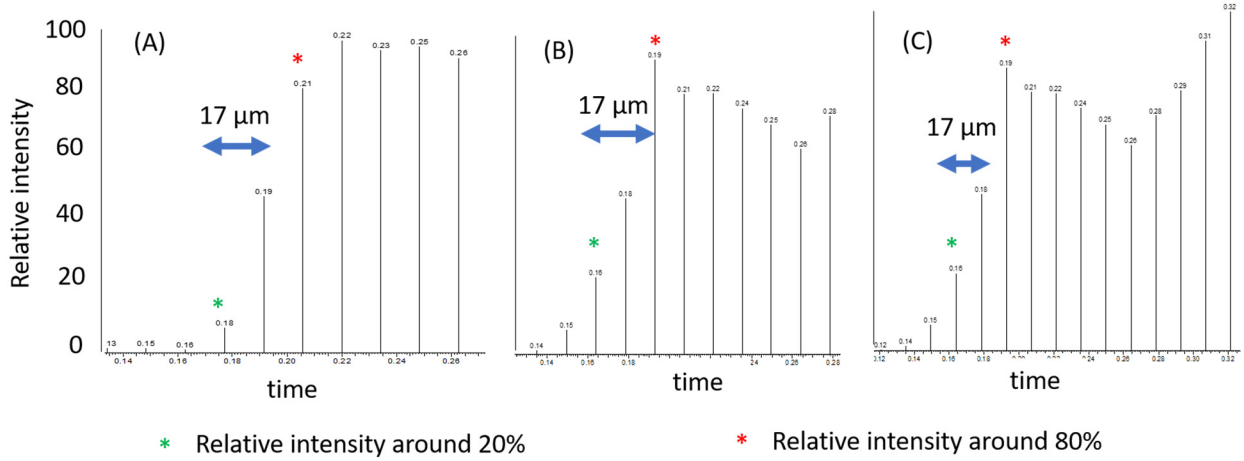

Figure S8. Characterization of the spatial resolution of MS images. The relative ion intensities of ion $[PC(36:1) + H]^+$ in three representative line scans in a MS image (Figure 2). The spatial resolution was determined on the distance with the relative ion intensities change from 20% to 80% (Reference #54).

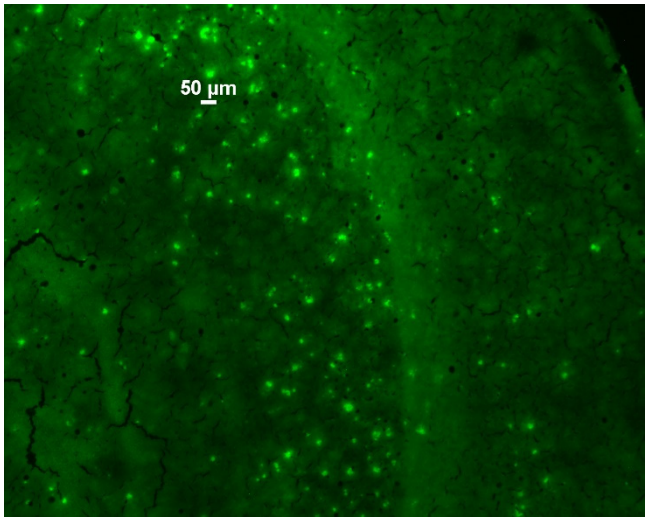

Figure S9. Stained slice of mouse brain with Alzheimer Disease. The sizes of most plaques (green bright dots) are smaller than 50µm.

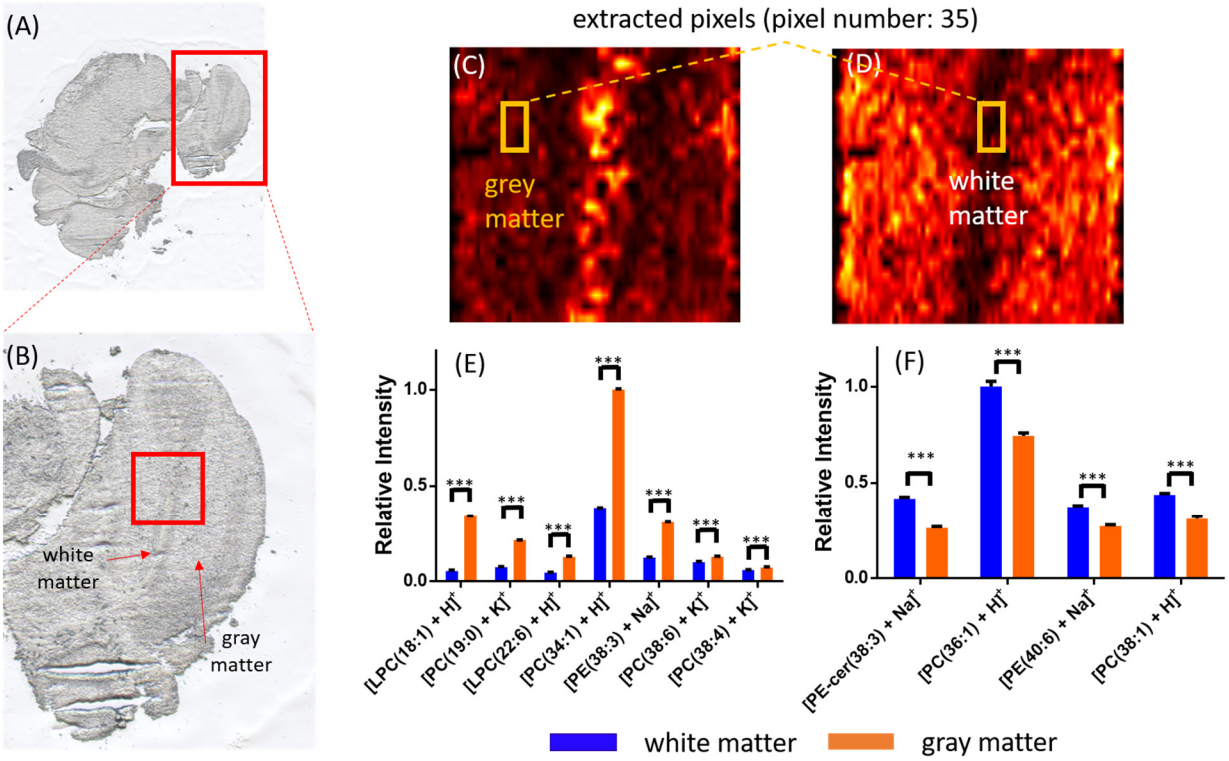

Figure S10. Experimental results from the control group. Bright-field microscopy image of (A) a control mouse brain and the zoomed-in region. MS images of (C) $[PC(36:1) + H]^+$ and (D) $[PC(34:1) + H]^+$. Metabolites with relatively higher abundances in (E) the gray matter and (F) white matter.

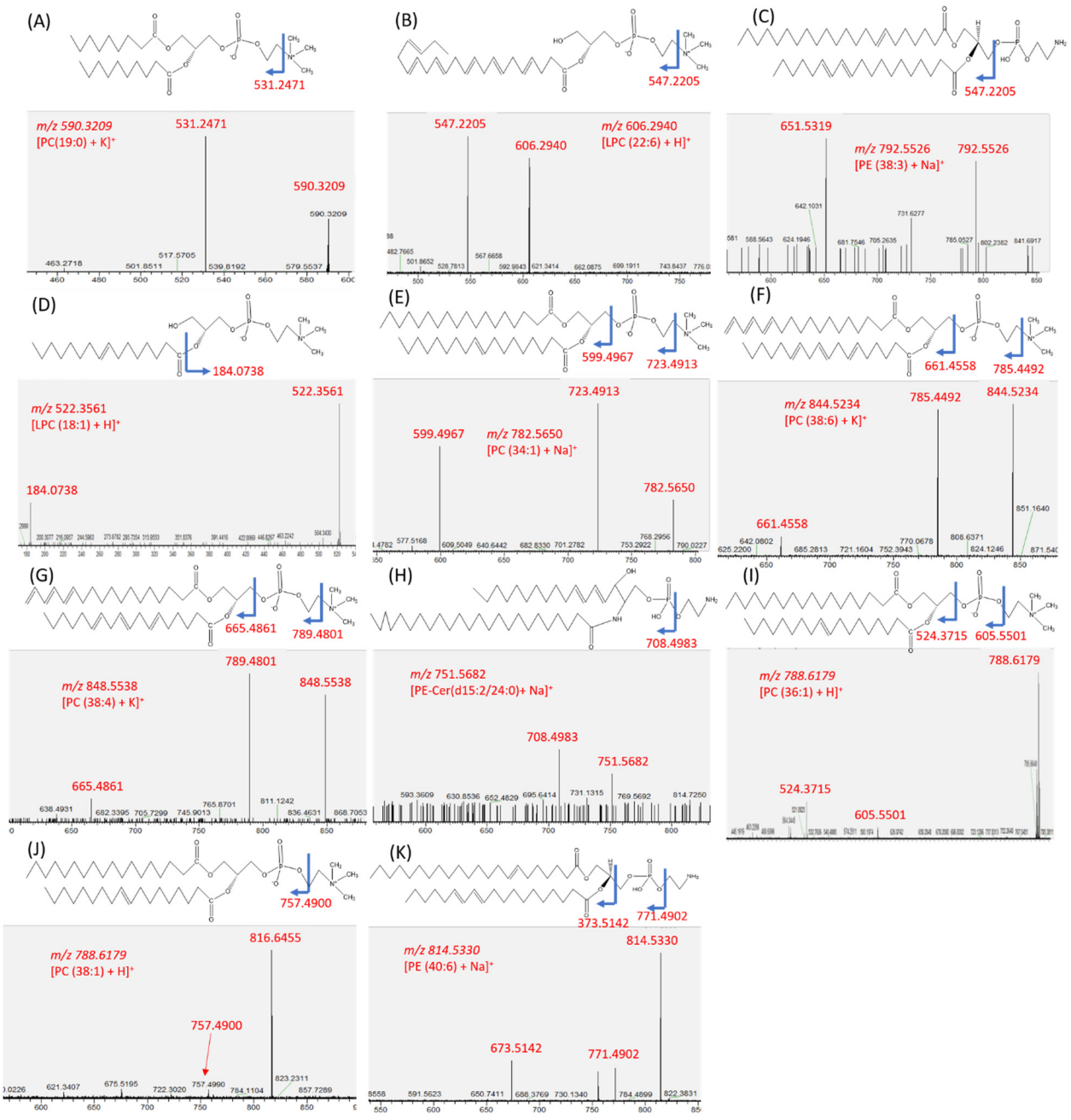

Figure S11. MS/MS analysis of selected metabolites in Figure S10 (positive ion mode), including (A) $[PC(19:0) + k]^+$, (B) $[LPC(22:6) + H]^+$, (C) $[PE(38:3) + Na]^+$, (D) $[LPC(18:1) +H]^+$, (E) $[PC(34:1) + Na]^+$, (F) $[PC(38:6) + K]^+$, (G) $[PC(38:4) + K]^+$, (H) $[PE\text{-}Cer(d15:2/24:0) + Na]^+$, (I) $[PC(36:1 + H)]^+$, (J) $[LPC(38:1) + H]^+$, (K) $[PE(40:6) + Na]^+$ (All MS/MS spectra were compared with online databases METLIN).

Supplementary Tables:

Table S1. Pixel selection in Aβ plaques and their surrounding regions from fused images.

Regions	Positive Ion Mode			Negative Ion Mode	
	1	2	3	1	2
Aβ	15	15	15	15	15
Surrounding	30	30	30	20	20

Table S2. Metabolites with significantly different abundances in Aβ plaques and their surrounding regions (positive ion mode).

m/z	Assignment*	Relative Intensity (plaque)	Relative Intensity (surrounding)
203.2225	$[Spermine + H]^+$	1.2×10^{-1}	1.2×10^{-2}
327.2286	$[Arachidonic\ acid + H]^+$	9.8×10^{-2}	4.3×10^{-2}
482.3241	$[LPC(15:0) + H]^+$	7.8×10^{-3}	1.5×10^{-3}
496.3381	$[LPC(16:0) + H]^+$	2.4×10^{-2}	1.5×10^{-2}
509.2242	$[LPG(15:0) + H]^+$	2.3×10^{-2}	2.6×10^{-3}
522.3536	$[LPC(18:1) + H]^+$	1.9×10^{-3}	1.2×10^{-3}
524.3696	$[LPC(18:0) + H]^+$	1.2×10^{-2}	3.1×10^{-3}
526.2912	$[LPE(22:6) + H]^+$	1.3×10^{-2}	8.0×10^{-3}
537.3532	$[PA(24:0) + H]^+$	3.9×10^{-3}	7.2 X 10-4
606.2936	$[LPC(22:6) + H]^+$	6.2×10^{-3}	3.3×10^{-3}
814.5233	$[PE(40:0) + H]^+$	1.2×10^{-2}	1.4×10^{-3}

*The assignment was based on the tandem mass spectra (MS/MS) and compared with online database Metlin. (LPC: lysophosphatidylcholines, LPG: lysophosphatidylglycerol, LPE: lysophosphatidylethanol, PA: Phosphatidic acids, PE: phosphatidylethanol)

Table S3. Metabolites with significantly different abundances in Aβ plaques and their surrounding regions (negative ion mode).

m/z	Assignment*	Relative Intensity (plaque)	Relative Intensity (surrounding)
133.0118	$[Malic\ acid - H]^-$	8.5×10^{-3}	1.08×10^{-2}
145.0431	$[Glutamine - H]^-$	8.4×10^{-4}	1.2×10^{-3}
132.0277	$[Aspartic\ acid - H]^-$	1.6×10^{-2}	6.5×10^{-2}
130.0513	$[(5\text{-}Aminolevulinic\ acid) - H]^-$	1.6×10^{-3}	2.2×10^{-3}
327.2323	$[(Docosahexaenoic\ acid) - H]^-$	1.4×10^{-2}	2.2×10^{-2}
151.0253	$[(Xanthine) - H]^-$	4.0×10^{-3}	1.2×10^{-2}
147.0452	$[(Phenylalanine) - H]^-$	2.3×10^{-3}	2.8×10^{-3}

*The assignment was based on the tandem mass spectra (MS/MS) and compared with online database METLIN.

Table S4. Metabolites illustrated in Figure 2 and Figure 6.

m/z	Assignment*	Ion mode
788.6197	$[PC(36:1) + H]^+$	Positive
848.5534	$[PC(37:6) + H]^+$	Positive
844.5218	$[PC(38:6) + K]^+$	Positive
832.5792	$[PC(38:4) + H]^+$	Positive
251.1065	$[Dodecenoic\ acid + K - 2H]^-$	Negative
309.2514	$[PA(O\text{-}32:0) - 2H]^{2-}$	Negative

*The assignment was based on the tandem mass spectra (MS/MS) and compared with online database METLIN. m/z 251.1065 and m/z 309.2514 were not identified due to their inadequate ion intensities. (PC: phosphatidylcholines, PA: phosphatidic acids).